Influence of Noise on the Results of Rigid Registration of Segmented Ovarian Volumes Using Spherical Correlation in Frequency Domain

BORIS CIGALE, DAMJAN ZAZULA
Faculty of Electrical Engineering and Computer Science
University of Maribor
Smetanova ulica 17, Maribor
SLOVENIA
boris.cigale@uni-mb.si http://storm.uni-mb.si

Abstract: - The influence of noise on the results of rigid registration of segmented ultrasound volumes is studied in this paper. Binary volumes result from a segmentation of ovarian ultrasound volumes. Rigid registration is preformed in frequency domain, where the rotation and translation can be calculated separately. The calculation of rotation is done using the amplitude spectrum and sphere correlation. The method was tested on pairs of synthetic volumes where ovarian follicles in one volume were altered and, thus, simulated different kinds of noise (non-rigid changes) characteristic for segmented volumes. We systematically assessed the performance of our registration algorithm by changing the number of follicles, their position, orientation and size. Hundred volume pairs were involved in each experiment. The method proved sensitive to the change of follicle size but resistive to all other kinds of destruction we simulated.

Key-Words: - image registration, rigid registration in frequency domain, spherical correlation

1 Introduction

Automated assessment of growth of structures given in 3D ultrasound images is a useful application which can relieve medical personnel of time-consuming and error-prone work. The algorithm presented in this paper is a part of our application for the detection and growth assessment of ovarian follicles.

The whole process of growth assessment can be divided into several steps. In the first step the centres of gravity in follicles are detected and their shapes are outlined in each ultrasound volume [1-4].

In the second step a rigid transformation which registers segmented volumes is calculated. This means a basis for the growth assessment. Registered volumes are, afterwards, additionally processed by elastic registration [5], which fine tunes the results.

Final step compares registered volumes and the follicle intersections are calculated. Intersections show a possible similarity of the structures.

The tested rigid registration works in frequency domain, as described in next section. The algorithm is described in Section 3. The efficiency of the algorithm is tested and discussed in Section 4, while Section 5 concludes the paper.

2 Rigid registration in frequency domain

Rigid registration uses rigid transformation which consists of translation and rotation. Rigid registration methods that are based on the frequency-domain transform are especially interesting because of the Fourier shift theorem. The theorem provides a mathematical tool to divide the problem of finding rigid transformation into two separate problems of finding translation and rotation.

2.1 Translation

Two volumes $\mathbf{V_1}$ and $\mathbf{V_2}$ are translated by vector $\mathbf{t}=(t_x,t_y,t_z)$ if the following relationship holds:

$$\mathbf{V}_2(x,y,z) = \mathbf{V_1}(x-t_x, y-t_y, z-t_z). \tag{1}$$

Cross-correlation [6] $\mathbf{R_{v1v2}(t)}$ is often used to detect such translation. Maximum value of argument $\mathbf{t}$ in $\mathbf{R_{v1v2}(t)}$ indicates the approximate translation parameter. Proceeding by the Fourier transform of this cross-correlation, the so called Cross Power Spectral Density Function is calculated as:

$$\mathbf{G_{v1v2}}(\xi,\nu,\zeta) = \iiint \mathbf{R_{v1v2}(t)}\, e^{-j2\pi(\xi t_x + \nu t_y + \zeta t_z)} dt_x dt_y dt_z. \tag{2}$$

If the inverse Fourier transform is applied to Eq. (2), one can easily get the cross-correlation values. In [7] it was shown that better results are obtained when a generalized cross-correlation method is used if volumes are corrupted by noise. In this case $\mathbf{G_{v1v2}}(\xi,\nu,\zeta)$ is multiplied by a general frequency weighting function

$\psi_g(\xi,\nu,\zeta)$. We deal with phase correlation if $\psi_g(\xi,\nu,\zeta)$ equals [7, 8]:

$$\psi_g(\xi,\nu,\zeta) = \frac{1}{\left|\mathbf{G}_{\mathbf{v1v2}}(\xi,\nu,\zeta)\right|}. \tag{3}$$

The abovementioned theory can be condensed into the following algorithm for the translation detection. Fourier transforms $\mathbf{\Psi_1}$ and $\mathbf{\Psi_2}$ are computed for $\mathbf{V_1}$ and $\mathbf{V_2}$, respectively. Cross power spectrum retains only the information about phase differences between $\mathbf{V_1}$ and $\mathbf{V_2}$ and can be calculated using Eqs. (2) and (3) as follows:

$$\mathbf{\Phi}(\xi,\nu,\zeta) = \frac{\mathbf{\Psi_1}(\xi,\nu,\zeta)\,\mathbf{\Psi_2}^*(\xi,\nu,\zeta)}{\left|\mathbf{\Psi_1}(\xi,\nu,\zeta)\right|\left|\mathbf{\Psi_2}(\xi,\nu,\zeta)\right|}, \tag{4}$$

where * denotes complex conjugate. Translation equals the position of maximum value in the result of the inverse Fourier transform of $\mathbf{\Phi}(\xi,\nu,\zeta)$.

2.2 Fourier shift theorem

Fourier shift theorem states that translation of the volume in the spatial domain influences just the phase of Fourier transform [9]. If $\mathbf{V_1}$ and $\mathbf{V_2}$ are related by Eq. (1), their Fourier transforms $\mathbf{\Psi_1}$ and $\mathbf{\Psi_2}$ yield:

$$\mathbf{\Psi_2}(\xi,\nu,\zeta) = e^{j2\pi(\xi t_x + \nu t_y + \zeta t_z)}\,\mathbf{\Psi_1}(\xi,\nu,\zeta). \tag{5}$$

If only the frequency-domain amplitudes are observed, the following equality holds true:

$$\left|\mathbf{\Psi_2}(\xi,\nu,\zeta)\right| = \left|\mathbf{\Psi_1}(\xi,\nu,\zeta)\right|. \tag{6}$$

Eq. (6) shows that translation does not influence the amplitude spectrum, thus, in the case of rigid transforms the amplitude spectrum is influenced just by rotation.

2.3 Rotation

Given two volumes $\mathbf{V_1}$ and $\mathbf{V_2}$ that are related by translation vector $\mathbf{t}=(t_x,t_y,t_z)$ and rotation matrix $\mathbf{R}$, the point $\mathbf{p}=(x,y,z)$ from $\mathbf{V_1}$ is linked with the corresponding point in $\mathbf{V_2}$ by:

$$\mathbf{V}_2(\mathbf{p}) = \mathbf{V_1}(\mathbf{Rp}-\mathbf{t}). \tag{7}$$

In frequency domain, the two volumes are related by the following equation:

$$\mathbf{\Psi_2}(\mathbf{k}) = e^{j2\pi\mathbf{k}^T\mathbf{R}^{-1}\mathbf{t}}\,\mathbf{\Psi_1}(\mathbf{Rk}), \tag{8}$$

where $\mathbf{k}$ denotes frequencies (ξ,ν,ζ). The relationship of amplitude spectra is the following:

$$\left|\mathbf{\Psi_2}(\mathbf{k})\right| = \left|\mathbf{\Psi_1}(\mathbf{Rk})\right|. \tag{9}$$

Eq. (9) proves that amplitude spectra are influenced only by rotation. Many algorithms exist for determining the rotation, however they mainly work in 2D [8]. An interesting approach was published in [10]. It is based on eigenvectors, nevertheless it turned out to be quite noise-sensitive in our experiments.

2.4 Detection of rotation parameters using spherical cross-correlation

We propose a detection of rotation in the amplitude spectrum by using spherical cross-correlation. Denote the amplitude spectra of $|\mathbf{\Psi_1}|$ and $|\mathbf{\Psi_2}|$ by $\mathbf{\Xi_1}$ and $\mathbf{\Xi_2}$, respectively. Referring to Eq. (9), $\mathbf{\Xi_2}(\mathbf{k}) = \mathbf{\Xi_1}(\mathbf{Rk})$.

It is trivial to show that the Euclidian distance between the frequencies $\mathbf{k}$ and (0, 0, 0) equals the Euclidian distance between the frequencies $\mathbf{Rk}$ and (0, 0, 0). This property changes the problem of finding the rotation using the amplitude spectrum to the problem of calculating spherical cross-correlation, since all frequencies with the same Euclidian distance form a sphere. After spherical cross-correlation computed, the rotation matrix $\mathbf{R}$ can be easily identified by the position of a maximum in correlation. We write more about how to do this in Section 3.

2.5 Correlation based on SO(3) Fourier Transform

SO(3) denotes a group of rotations about the origin in 3D. Rotations are represented by 3×3 matrices with determinant 1, or with Euler angles α, β, γ, where $0 \le \alpha, \gamma \le 2\pi$ and $0 \le \beta \le \pi$. Any element $\mathbf{G}$ from SO(3) can be expressed with those angles as [11]:

$$\mathbf{G} = g(\alpha,\beta,\gamma) = \mathbf{R_z}(\alpha)\,\mathbf{R_y}(\beta)\,\mathbf{R_z}(\gamma) \tag{10}$$

where $\mathbf{R_z}(a)$ and $\mathbf{R_y}(\beta)$ stand for the rotation matrices around the z and y axes, respectively.

Denote two functions on a sphere as $f(\omega)$ and $h(\omega)$, where $\omega=(\theta,\varphi)$ stands for spherical coordinates. To each $\mathbf{G}$ we can associate linear operator $\Lambda_\mathbf{G}$ which acts on $h(\omega)$:

$$\Lambda_\mathbf{G} h(\omega) = h(\mathbf{G}^{-1}\omega) \tag{11}$$

We can define the correlation of $f(\omega)$ and $h(\omega)$ as:

$$K(\alpha,\beta,\gamma) = \int_{\omega\in S^2} f(\omega)\Lambda^*_{g(\alpha,\beta,\gamma)}h^*(\omega)d(\omega) \tag{12}$$

where * denotes complex conjugates.

As in planar cases, the correlation on sphere can be performed in frequency domain by using spherical Fourier transform of *f(ω)* and *h(ω)*. To do this we used the algorithm published in [11], where also the method's details are revealed.

3 Registration algorithm

In this section we describe the proposed algorithm for a registration in frequency domain. The algorithm runs on two input volumes $\mathbf{V_1}$ and $\mathbf{V_2}$. We assume both volumes binary, as they exit the segmentation step, however the procedure should also work with volumes comprising grey-valued voxels.

A bounding box for each volume is determined to decrease space and time complexity of the algorithm. Then we calculate 3D Fourier transform for $\mathbf{V_1}$ and $\mathbf{V_2}$ to get $\mathbf{\Psi_1}$ and $\mathbf{\Psi_2}$. It is important that $\mathbf{\Psi_1}$ and $\mathbf{\Psi_2}$ are of the same size, therefore we pad the smaller volume by zeroes.

We calculate the amplitude spectra $\mathbf{\Xi_1}$ and $\mathbf{\Xi_2}$ for $|\mathbf{\Psi_1}|$ and $|\mathbf{\Psi_2}|$, respectively. Both $\mathbf{\Xi_1}$ and $\mathbf{\Xi_2}$ are normalized by their DC components: $\mathbf{\Xi_1}/\mathbf{\Xi_1}(0)$ and $\mathbf{\Xi_2}/\mathbf{\Xi_2}(0)$.

Then we calculate spherical cross-correlations for various distances from frequency 0. Let $\mathbf{o}_r$ designate the vector of spherical cross-correlation at distance r, obtained by using the computer program disclosed in [11]. Each vector $\mathbf{o}_r$ is normalized by its maximum value. Vectors $\mathbf{o}_r$ at various distances are summed up. Denote the resulting vector by $\mathbf{o}$.

Indices of the vector's elements can be expressed by Euler's angles that describe the rotation matrix. It should be stressed that the highest value in vector $\mathbf{o}$ does not automatically sort out the best rotation matrix. Remember that the amplitude spectrum is symmetric, therefore an ambiguous rotation in spatial domain can be obtained. Such false rotations are always rotated by 90 degrees from the correct ones.

To find the proper rotation we further test the 24 rotations with highest spherical cross-correlations. Any rotation $\mathbf{R}_i$ is tested by the following procedure. Volume $\mathbf{V_1}$ is initially rotated by $\mathbf{R_i}$. If the rotation is correct, one can obtain translation $\mathbf{t_i}$ by calculating cross power spectrum as described in 2.1. Registration accuracy is estimated by a ratio ρ that compares the intersection volume of the two registered volumes $\mathbf{V_{1R}}$ and $\mathbf{V_2}$ to the final volume $\mathbf{V_2}$.

The obtained rigid transformation is finally improved by applying the ICP (Iterative Closest Point) algorithm [12], like in [13]. The ICP algorithm is widely used for rigid alignment of two clouds of points when an initial estimate of the relative pose is known. It iteratively revises the transformation needed to minimize the distance between the points.

4 Simulation results

4.1 Model description

The efficiency of the algorithm was tested on binary synthetic 3D volumes. The volumes simulate outputs of our follicle segmentation algorithm which process ultrasound (US) volumes [1-4], like one depicted in Fig. 1.

A follicle in 3D US volumes is seen as a spherical homogenous region whose average greyness is darker than the surroundings. There can be more than one follicle in such image, especially when the patient receives hormone therapy. Size of follicles differ, the largest follicles are called dominant follicles.

Our goal was to assess the growth of the individual follicles. The crucial step in this assessment is a successful registration of two volumes that belong to the same patient and are acquired in consecutive examinations.

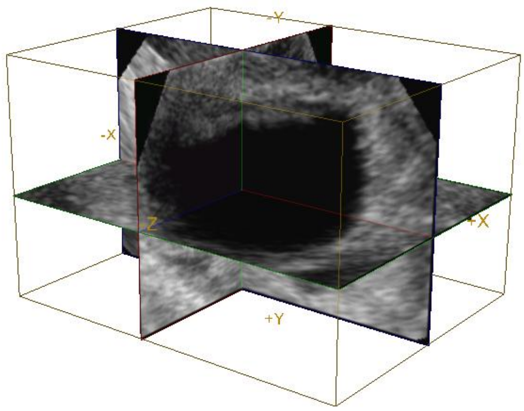

Figure 1: 3D view of an ultrasound volume

Our model consists of two 3D volumes, filled with ellipsoids that simulate the segmented follicles. Each of volumes represents one of the examinations, and since the position of ultrasound probe changes from one examination to another, we introduced different points of view that are simulated by rigidly transforming the modelled volumes. Due to the fact that real follicles exhibit considerable dynamics by their growth, decline, appearance and disappearance, we simulate this dynamics too.

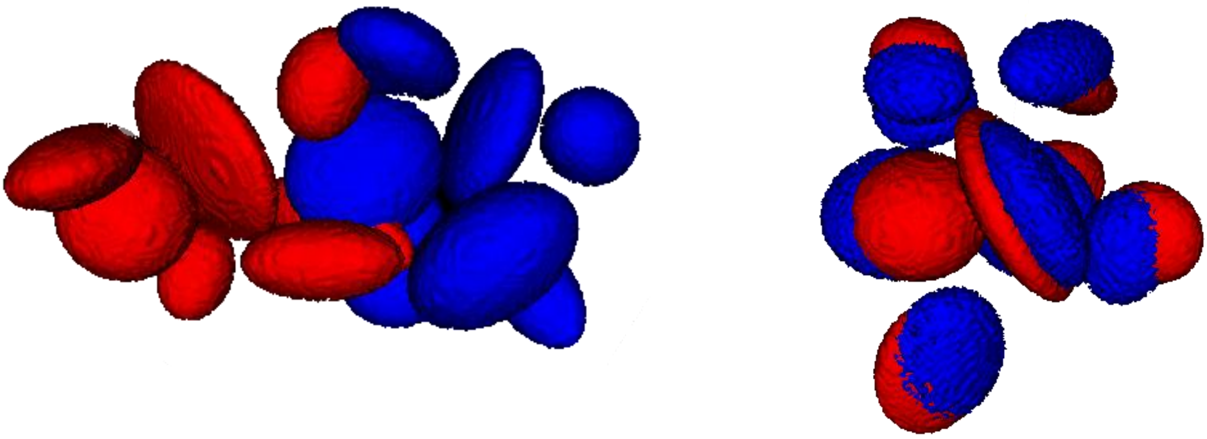

(a) (b)

Figure 2: Simulated volumes $\mathbf{V_1}$ and $\mathbf{V_2}$ before (a) and after (b) registration

We began by creating the volume $\mathbf{V_1}$ of dimensions 150×150×150 voxels. Inside the volume, we placed 8 ellipsoids whose size, position and rotation is randomly chosen (uniform distribution) by the following rules. The whole ellipsoid must fit into the volume, the ellipsoid radii (*a*, *b, c*) are set within the range of [10, 30] voxels. Each ellipsoid is randomly rotated by Euler's angles α, β, γ in the range of [-0.5, 0.5] radians (-29 to 29 degrees). We took precautions that ellipsoids do not intersect.

For volume $\mathbf{V_2}$ we firstly created a random rigid transform matrix that simulates a rigid transform. To simulate the dynamics of follicle growth the volume $\mathbf{V_2}$ was created by altering the parameters for $\mathbf{V_1}$.

Not all ellipsoids from $\mathbf{V_1}$ were preserved in $\mathbf{V_2}$; to simulate real dynamics we deleted at most 3 of them. This simulates disappearance of follicles and, at the same time, the errors of not detected follicles due to a bad segmentation. Parameters of the remaining ellipsoids were altered. Centres of gravity in each ellipsoid were randomly changed for at most 10 voxels in each coordinate axis (maximum Euclidan distance of two such centres is therefore 17 voxels). This simulates displacement of follicles. The radii *a*, *b*, *c* of the ellipsoid were also individually and randomly changed by 20 % (e.g., for the radius *a* of 30 voxels, the new size is in the range of [24, 36] voxels). This simulates the follicle growth and decline. To simulate displacement, each ellipsoid was randomly rotated in a range from -15 to 15 degrees in each Euler's angle. To simulate new follicles, we randomly added at most 3 new ellipsoids.

When creating $\mathbf{V_2}$ we did not take any special precautions for ellipsoids not to intersect, so that they usually do. This simulates the behaviour of segmentation algorithms that tend to connect follicles lying close together in US volume. Simulated volumes $\mathbf{V_1}$ and $\mathbf{V_2}$ are exemplified by Fig. 2.

We showed in [14] that the follicle dynamics influence the results of our registration algorithm. Therefore we made several experiments in which we separately altered parameters for follicles in $\mathbf{V_2}$. We treat such alternation of parameters as a noise, since it is seen as such from the perspective of rigid transform.

4.2 Registration results

In each experiment we tested our registration method on 100 pairs of synthetic binary volumes. When calculating spherical correlation the radial distances between [10, 30] voxels were used.

We estimated the alignment of volumes after every registration. The ratio ρ compares the intersection volume of the two registered volumes $\mathbf{V_{1R}}$ and $\mathbf{V_2}$ to the final volume $\mathbf{V_2}$. In an ideal case this ratio would be 1. Three different ratios were calculated: ρ_k denotes the results obtained by the same transformation as used in the model creation (ρ_k would be 1 if we did not change the parameters of ellipsoids); ρ_f denotes the results obtained just by using spherical cross-correlation, without the last step that utilizes ICP; ρ_i denotes the final result after all steps of our registration algorithm.

We also compared the difference between the rotation used in the model and rotation calculated by our algorithm. Rotation in 3D can be described with 3 Euler's angles. In such a way it is difficult to compare two different rotations, therefore we expressed rotations with quaternions. We denote the spatial angle between quaternions by Θ. We expect that angle Θ is small.

The result was also evaluated by the difference between the translations. We calculated the Euclidian distance between the translation used in the model and the translation calculated by our algorithm. We denote this distance by *d*. We expect that distance *d* is small.

4.2.1 Ideal case

In the first experiment we study the ideal case, where the only difference between $\mathbf{V_1}$ and $\mathbf{V_2}$ was a random rigid transform. In Fig. 3, the results for all 100 pair of volumes are depicted. The average ratio ρ_k is 0.99 (std. 0.01), average ratio ρ_f is 0.87 (std. 0.04) and average ratio ρ_i is 0.94 (std 0.02). The average angle Θ between known and calculated rotation is 3.10 (std 1.10) degrees and average distance d between known and calculated translation is 5.17 (std 2.39) voxels.

The obtained results show that our registration algorithm performs very well in ideal case.

4.2.2 New follicles

In the second experiment we tested how our algorithm performs in the case, when additional new follicles appear in $\mathbf{V_2}$. Otherwise, all follicles from $\mathbf{V_1}$ remain in $\mathbf{V_2}$. This simulates appearance of new follicles and, at the same time, the errors of wrongly detected follicles due to a bad segmentation. The number of additional follicles was random but limited to 3. Our automated registration case generator created a testing set in which we have 17 pairs of volumes with no new follicle added in $\mathbf{V_2}$, 40 pairs with 1 follicle added, 31 pairs with 2 follicles added, and 12 pairs with 3 follicles added. In Fig. 4, the results for all 100 pair of volumes are depicted. The average ratio ρ_k is 0.99 (std. 0.01), average ratio ρ_f is 0.85 (std. 0.06) and average ratio ρ_i is 0.93 (std 0.06). The average angle Θ between known and calculated rotation is 4.82 (std 18.27) degrees and average distance d between known and calculated translation is 7.60 (std 22.61) voxels.

In Fig. 4 we can see that our segmentation algorithm successfully registered 99 pairs of volumes, but was unsuccessful in one case. Only one additional follicle was added to $\mathbf{V_2}$ in that particular case. Nevertheless, we can conclude that the algorithm performs well when changes in the form of additional follicles are induced.

4.2.3 Missing follicles

In the third experiment we tested how missing follicles that exist in $\mathbf{V_1}$ but not in $\mathbf{V_2}$ influence the registration results. None of the new follicles appear in $\mathbf{V_2}$. This simulates disappearance of follicles due to their maturation cycle and, at the same time, the errors of not detected follicles due to a bad segmentation. The number of removed follicles was random but limited to 3. Our automated registration case generator created a testing set in which we have 26 pairs of volumes with no follicles removed from $\mathbf{V_2}$, 28 pairs with 1 follicle removed, 31 pairs with 2 follicles removed, and 15 pairs with 3 follicles removed. In Fig. 5, the results for all 100 pair of volumes are depicted. The average ratio ρ_k is 0.82 (std. 0.14), average ratio ρ_f is 0.72 (std. 0.13) and average ratio ρ_i is 0.78 (std 0.14). The average angle Θ between known and calculated rotation is 3.31 (std 1.39) degrees and average distance d between known and calculated translation is 5.60 (std 2.97) voxels.

The results prove our registration algorithm performs successfully even with missing follicles, since all test cases were correctly registered.

4.2.4 New and missing follicles

In the fourth experiment we tested how algorithm's performs when some new follicles appear in the second volume and some of follicles are also removed. The number of additional follicles was random but limited to 3. Our automated registration case generator created a testing set in which we have 18 pairs of volumes with no follicles added, 37 pairs with 1 follicle added, 29 pairs with 2 follicles added, and 16 pairs with 3 follicles added to $\mathbf{V_2}$. Similarly, the number of removed follicles was random and limited to 3. Our generator created a test set in which we have 15 pairs of volumes with no follicles removed from $\mathbf{V_2}$, 38 pairs with 1 follicle removed, 31 pairs with 2 follicles removed, and 16 pairs with 3 follicles removed. In Fig. 6, the results for all 100 pair of volumes are depicted. The average ratio ρ_k is 0.83 (std. 0.13), average ratio ρ_f is 0.72 (std. 0.13) and average ratio ρ_i is 0.78 (std 0.14). The average angle Θ between known and calculated rotation is 8.04 (std 26.86) degrees and average distance d between known and calculated translation is 12.86 (std 37.70) voxels.

Fig. 6 shows that our registration algorithm was unsuccessful in 3 cases out of 100. Only one additional follicle was added to $\mathbf{V_2}$ in all three particular cases. At the same time, 3 follicles were removed in two cases and 1 follicle in one case.

4.2.5 Displacement of follicles

In this experiment we tested how well our algorithm performs, when follicles move in the tissue. In order to do so, we randomly moved the centres of follicles in $\mathbf{V_2}$ for at most 10 voxels in each coordinate axis (maximal Euclidan distance of two such centres is therefore 17 voxels). In Fig. 7, the results for all 100 pair of volumes are depicted. The average ratio ρ_k is 0.63 (std. 0.05), average ratio ρ_f is 0.65 (std. 0.08) and average ratio ρ_i is 0.70 (std 0.07). The average angle Θ between known and calculated rotation is 9.00 (std 19.65) degrees and average distance d between known and calculated translation is 15.70 (std 25.49) voxels.

From the Fig. 7 it is clear that our registration algorithm was successful in registering 99 pairs of volumes, but was unsuccessful in one case. The average displacement of follicle in that particular case was 9.43

voxels (std. 2.12). However it is interesting that average ratio ρ_i is greater than ρ_k.

4.2.6 Rotation of follicles

To further test the displacement we tested how local rotation of follicles influences the results. Each ellipsoid in $\mathbf{V_2}$ was randomly rotated in a range from -15 to 15 degrees in each Euler's angle. In Fig. 8, the results for all 100 pair of volumes are depicted. The average ratio ρ_k is 0.96 (std. 0.01), average ratio ρ_f is 0.82 (std. 0.09) and average ratio ρ_i is 0.92 (std 0.04). The average angle Θ between known and calculated rotation is 4.37 (std 17.68) degrees and average distance *d* between known and calculated translation is 5.86 (std 12.96) voxels.

From the Fig. 8 it is clear that our registration algorithm was unsuccessful in only one case out of 100.

4.2.7 Follicles growth

In this experiment we tested how the growth and decline of follicles influence the results of our registration algorithm. Therefore the radii *a, b, c* of the ellipsoids in $\mathbf{V_2}$ were individually and randomly changed by 20 %. In Fig. 9, the results for all 100 pair of volumes are depicted. The average ratio ρ_k is 0.92 (std. 0.03), average ratio ρ_f is 0.68 (std. 0.18) and average ratio ρ_i is 0.82 (std 0.18). The average angle Θ between known and calculated rotation is 25.11 (std 54.85) degrees and average distance *d* between known and calculated translation is 33.84 (std 68.37) voxels.

From the Fig. 9 and calculated results it is clear that our registration algorithm performance is very poor when this type of noise is present. This can be explained by the fact that the change of the follicle size express in the change of the distance from frequency 0 in frequency domain.

4.2.8 All test cases combined

Finally, we combined all types of noise used in previous experiments. The number of additional and removed follicles in $\mathbf{V_2}$ was random but limited to 3. The centres of follicles in $\mathbf{V_2}$ were moved for at most 10 voxels in each coordinate axis. Each ellipsoid in $\mathbf{V_2}$ was randomly rotated in a range from -15 to 15 degrees and its size was randomly changed by 20 %. The results are depicted in Fig. 10. The average ratio ρ_k is 0.59 (std. 0.08), average ratio ρ_f is 0.44 (std. 0.10) and average ratio ρ_i is 0.51 (std 0.11). The average angle Θ between known and calculated rotation is 58.18 (std 66.05) degrees and average distance *d* between known and calculated translation is 84.17 (std 84.98) voxels.

Fig. 10 and calculated results show that our registration algorithm performance is poor, however from the previous experiments we can conclude that most of the errors originate form the problem of follicle growth.

4.3 Discussion

The results of the proposed registration method are in most cases comparable with the computations where the registration is based on known transformation parameters used for the simulation models creation. However, the experiments showed that our procedure has significant problems with the cases where the size of follicles changes. The results also show that the implementation of ICP improves the algorithm's performance, in particular its accuracy. This improvement was expected, since spherical cross-correlation is computed just for a limited, finite set of possible rotations.

5 Conclusions

We proposed and tested a novel algorithm for rigid registration of binary volumes in frequency domain. The most important part is the calculation of rotational parameters using the amplitude spectrum.

Translation was determined by spherical correlation. We applied an algorithm that calculates spherical cross-correlation by transforming spheres into the SO(3) frequency domain. We believe that the obtained results would be different if spherical cross-correlation were calculated by a different technique. Corresponding tests will be performed in the future.

We showed that the results are usually stable also in the noisy environment (non-rigid changes) where registered volumes are not entirely equal. We showed empirically that the biggest challenge to the registration algorithm is the change of the follicle size. Most probably this drawback must be attributed to the way we threat particular frequencies separately when calculating the rotations, therefore multiple frequencies should be observed simultaneously in the future.

References:

[1] B. Cigale, S. Šinjur, D. Zazula, *Automated Quantitative Assessment of Perifollicular Vascularization Using Power Doppler Ultrasound Images*, WSEAS Transactions on Computers, Vol. 9, No. 2, 2010, pp. 194-203.

[2] B. Cigale, S. Šinjur, D. Zazula, *Automated quantitive assessment of perifollicular vascularisation*, WSEAS CSECS '09, 2009, pp. 227-231.

[3] B. Cigale, D. Zazula, Segmentation of Ovarian Ultrasound Images Using Cellular Neural Networks,

International Journal of Pattern Recognition and Artificial Intelligence, Vol. 18, No. 4, 2004, pp. 563-581.

[4] B. Cigale, *A Multiscale Approach to Detection and Growth Assessment of Structures in 3D Ultrasound Volumes*, PhD Thesis, Faculty of Electrical engineering and Computer Science, Maribor, 2007.

[5] S. Šprager, B. Cigale, D. Zazula, *Estimation of Growth of Ovarian Follicles Using Rigid and Elastic Ultrasound Image Registration*, Proceedings of BIOSIGNALS 2010, Spain, 2010, pp. 333-338.

[6] A. Papoulis, *The Fourier Integral and Its Applications*, McGraw-Hill, 1962.

[7] C. Knapp, G. Carter, *The generalized correlation method for estimation of time delay*, IEEE Transactions on Acoustics, Speech and Signal Processing, Vol. 24, No. 4, 2003, pp. 320-327.

[8] S. B. Reddy, B. N. Chatterji, *An fft-based technique for translation, rotation, and scale-invariant image registration*, IEEE Transactions on Image Processing, Vol. 5, No. 8, 1996, pp. 1266-1271.

[9] S. W. Smith, *The Scientist and Engineer's Guide to Digital Signal Processing*, California Technical Publishing, 1999.

[10] L. Lucchese, G. Doretto, G. M. Cortelazzo, *A Frequency Domain Technique for Range Data Registration*, IEEE Trans. Pattern Anal. Mach. Intell., Vol. 24, No. 11, 2002, pp. 1468-1484.

[11] P. Kostelec, D. Rockmore, *FFT's on the rotation group, J. Fourier Anal. Appl.*, Vol. 14, 2008, pp. 145-179.

[12] S. Rusinkiewicz, M. Levoy, *Efficient variants of the ICP algorithm*, Third International Conference on 3D Digital Imaging and Modeling, 2001, pp. 145-152.

[13] C. T. Ferrero, S. Robla, E. G. Sarabia, J. R. LLata, *A Coarse-to-Fine Algorithm for 3D Registration based on Wavelet Decomposition*, WSEAS Transactions on Systems, Vol. 7, No. 7, 2008, pp. 655-664.

[14] B. Cigale, D. Zazula, *Rigid Registration of Segmented Volumes in Frequency Domain Using Spherical Correlation*, WSEAS MAMECTIS '10, pp. 234-238.

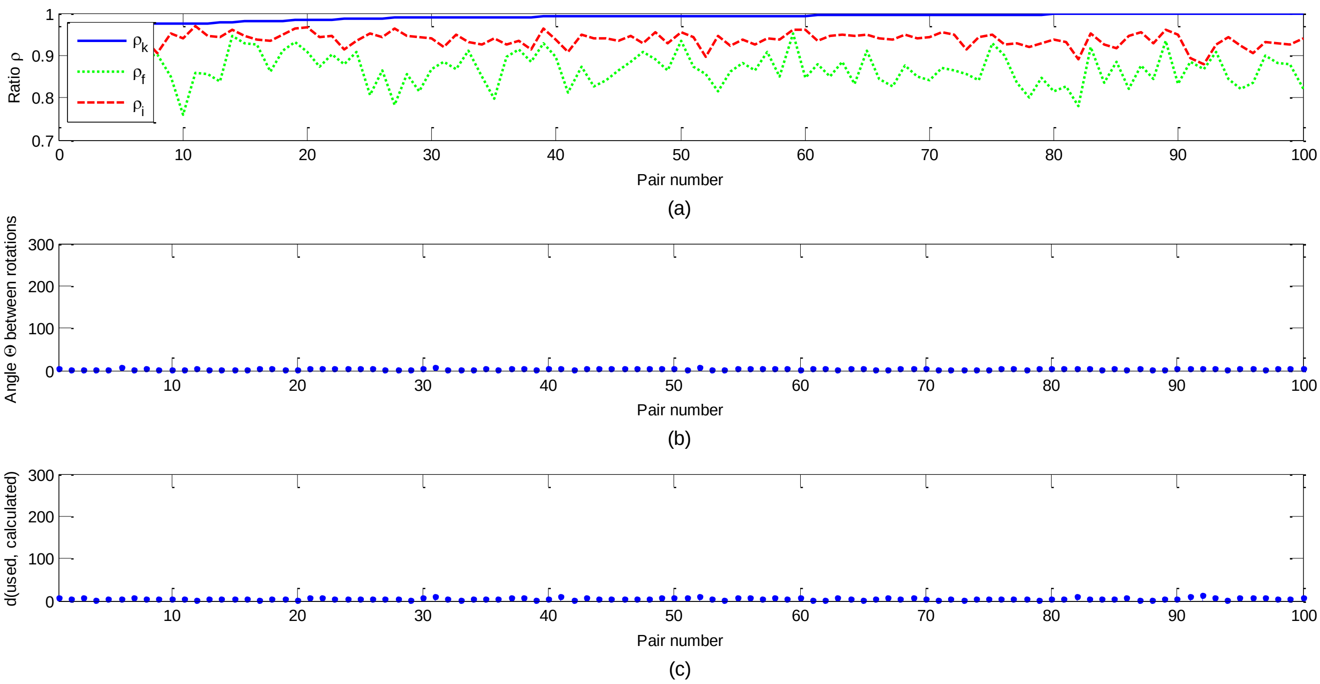

Figure 3: Registration accuracy in the ideal case: ρk denotes the results obtained by the same transformation parameters as used in the model creation, ρf denotes the results obtained just by using spherical correlation, without the last step that utilizes ICP; ρi denotes the final result after all steps of our registration algorithm (a). Angle Θ between known and calculated rotation (b). Distance *d* between known and calculated translation (c).

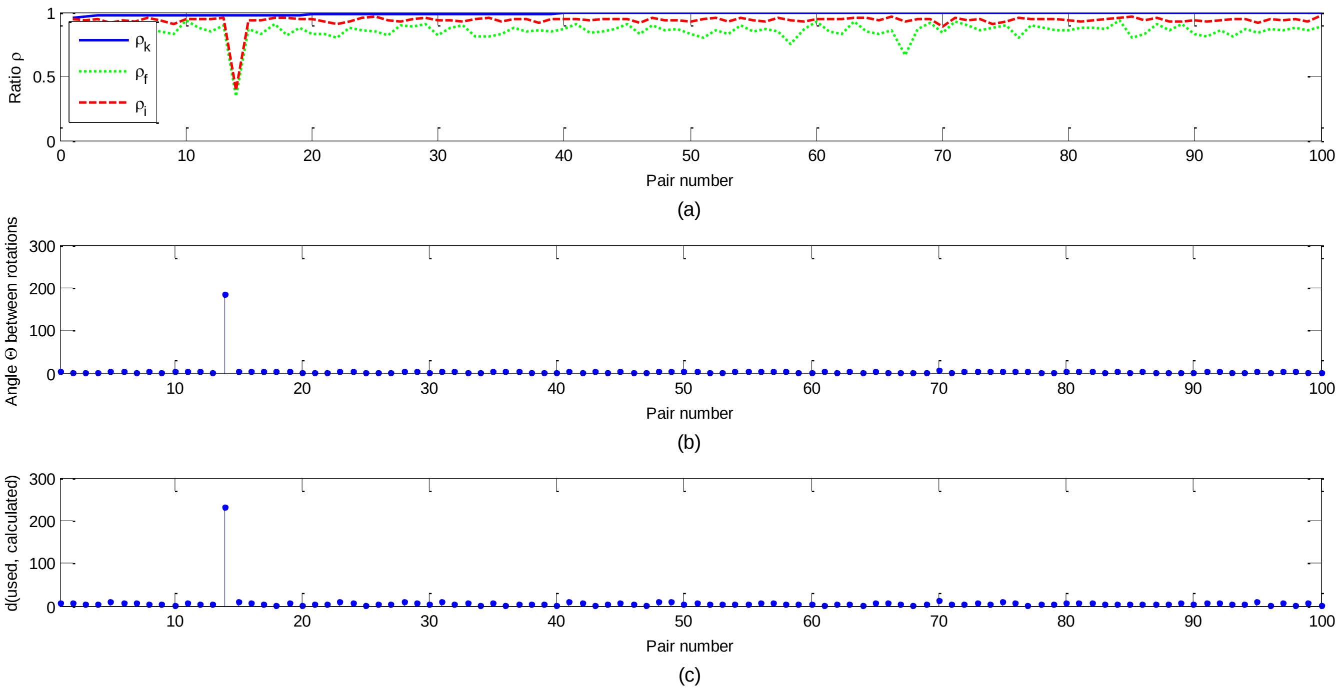

Figure 4: Registration accuracy in the case of appearing follicles: ρk denotes the results obtained by the same transformation parameters as used in the model creation, ρf denotes the results obtained just by using spherical correlation, without the last step that utilizes ICP; ρi denotes the final result after all steps of our registration algorithm (a). Angle Θ between known and calculated rotation (b). Distance *d* between known and calculated translation (c).

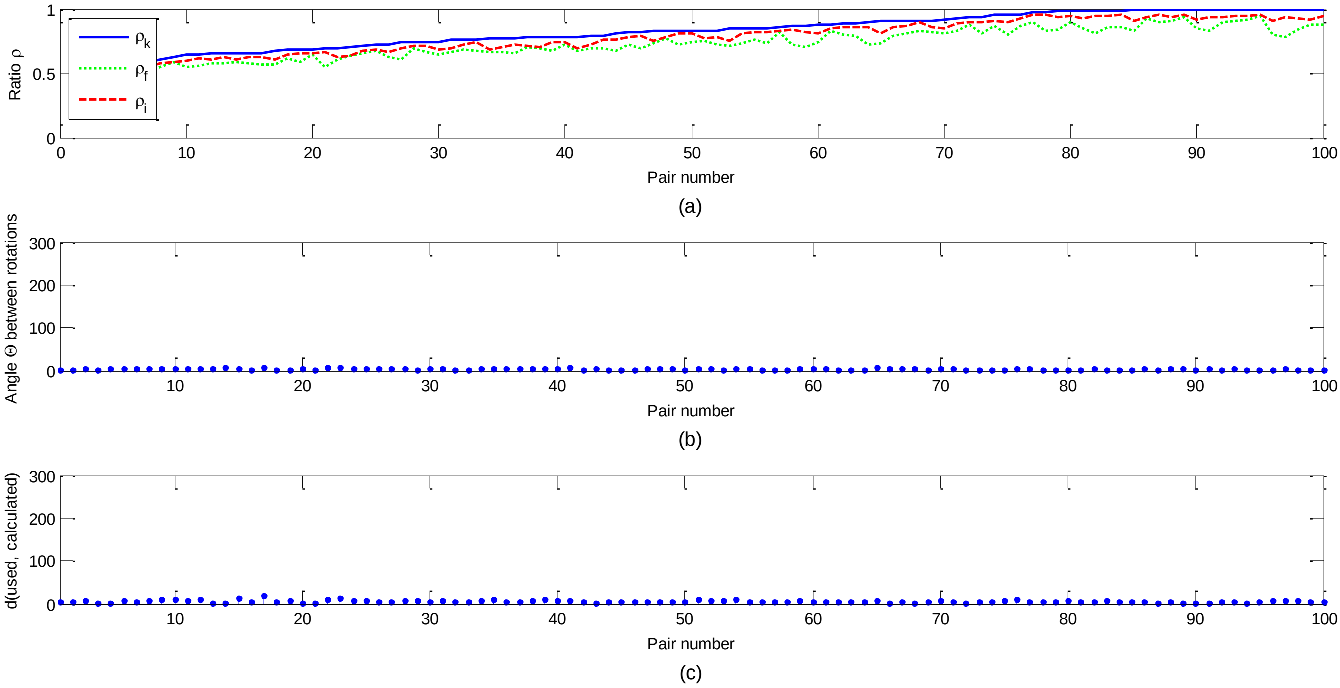

Figure 5: Registration accuracy for 100 volume pairs in the case of dissapearing follicles: ρk denotes the results obtained by the same transformation parameters as used in the model creation, ρf denotes the results obtained just by using spherical correlation, without the last step that utilizes ICP; ρi denotes the final result after all steps of our registration algorithm (a). Angle Θ between known and calculated rotation (b). Distance d between known and calculated translation (c).

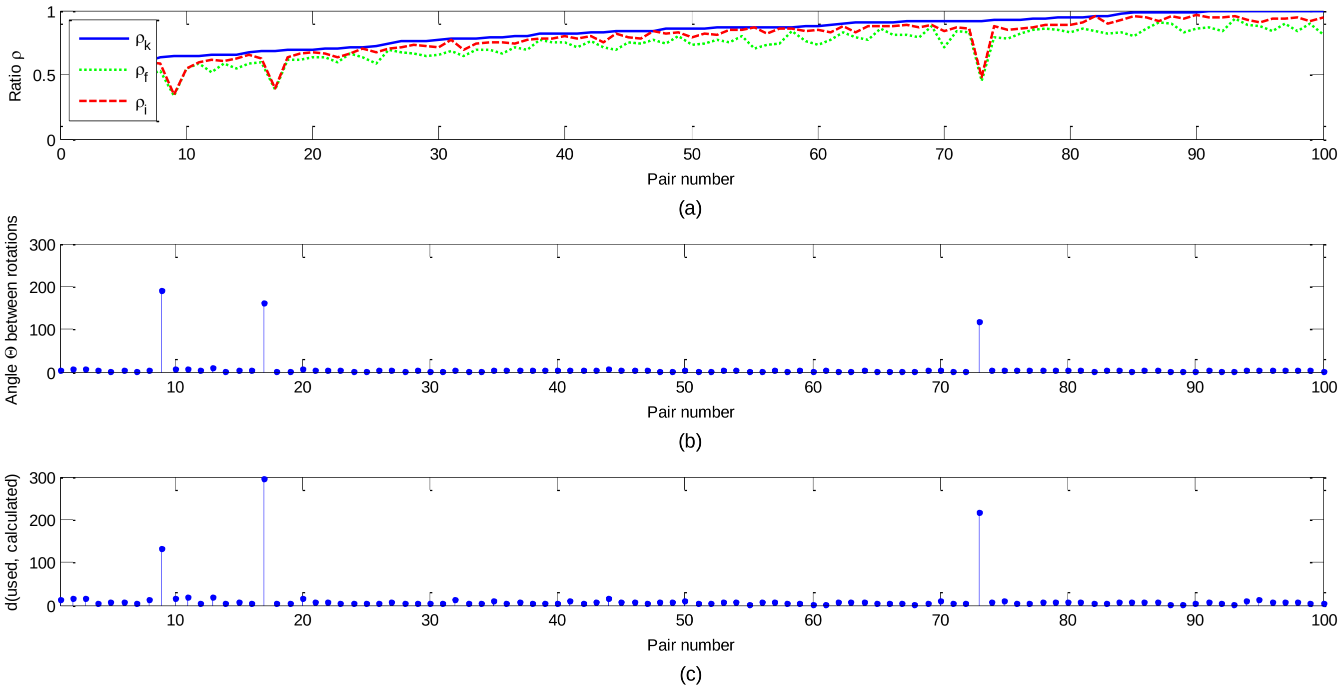

Figure 6: Registration accuracy for 100 volume pairs in the case of appearing and dissapearing follicles: ρk denotes the results obtained by the same transformation parameters as used in the model creation, ρf denotes the results obtained just by using spherical correlation, without the last step that utilizes ICP; ρi denotes the final result after all steps of our registration algorithm (a). Angle Θ between known and calculated rotation (b). Distance *d* between known and calculated translation (c).

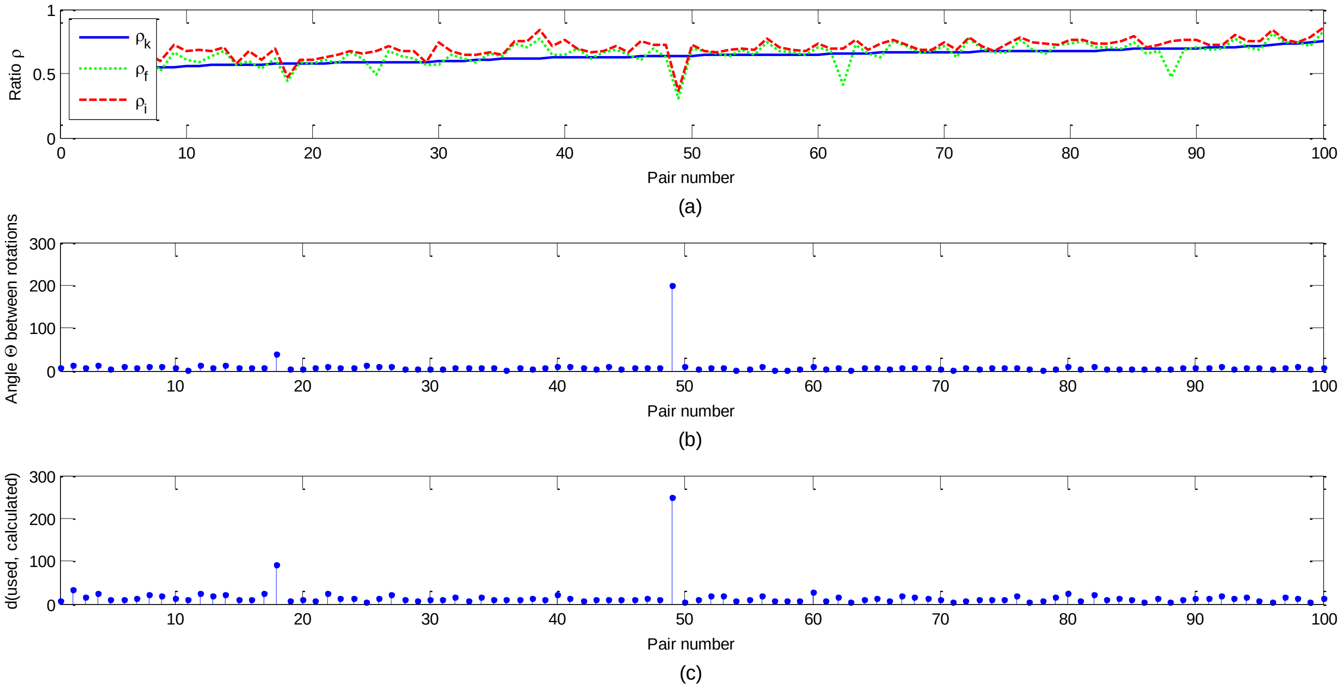

Figure 7: Registration accuracy for 100 volume pairs in the case of follicle displacement: ρk denotes the results obtained by the same transformation parameters as used in the model creation, ρf denotes the results obtained just by using spherical correlation, without the last step that utilizes ICP; ρi denotes the final result after all steps of our registration algorithm (a). Angle Θ between known and calculated rotation (b). Distance *d* between known and calculated translation (c).

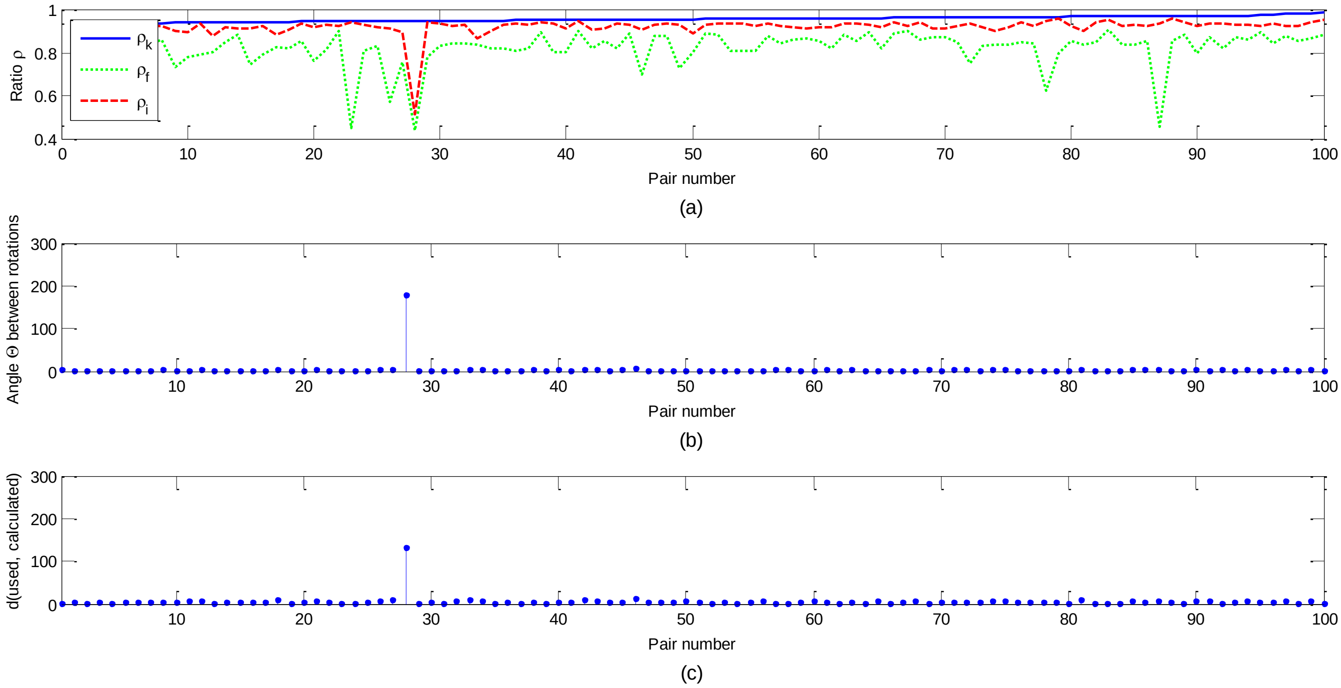

Figure 8: Registration accuracy for 100 volume pairs in the case of follicle rotation: ρk denotes the results obtained by the same transformation parameters as used in the model creation, ρf denotes the results obtained just by using spherical correlation, without the last step that utilizes ICP; ρi denotes the final result after all steps of our registration algorithm (a). Angle Θ between known and calculated rotation (b). Distance *d* between known and calculated translation (c).

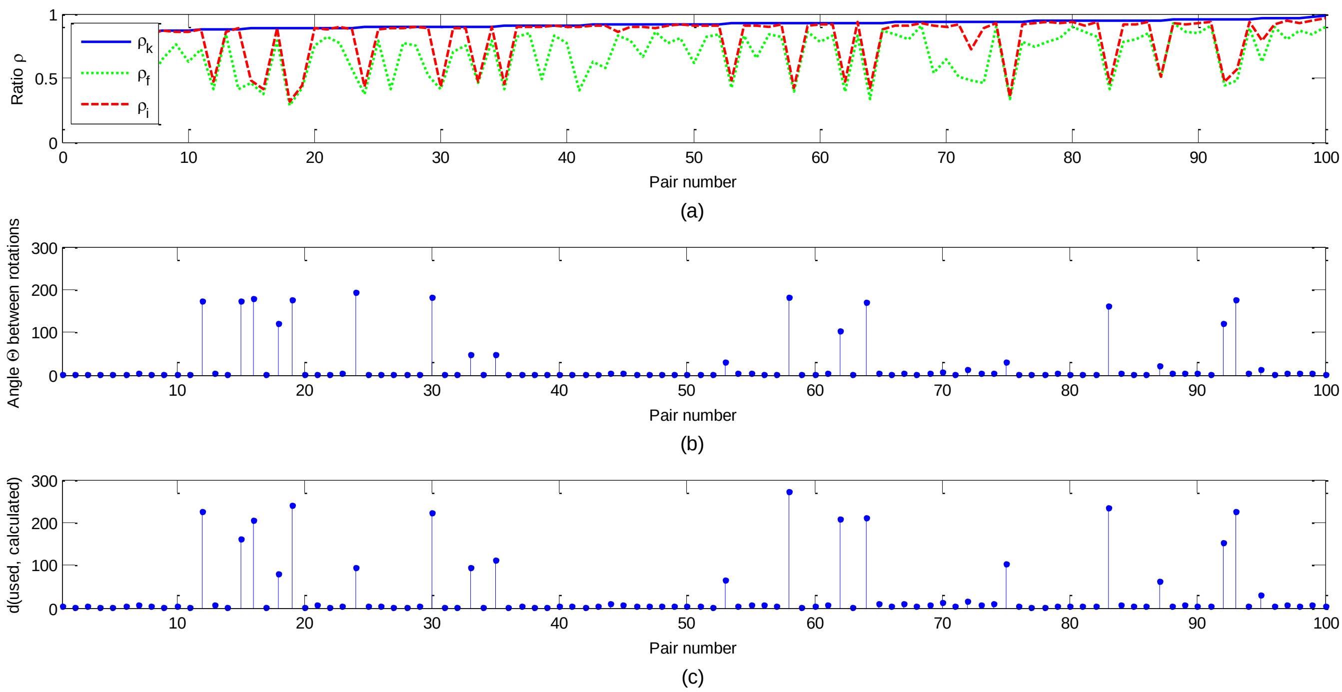

Figure 9: Registration accuracy for 100 volume pairs in the case of follicle growth: ρk denotes the results obtained by the same transformation parameters as used in the model creation, ρf denotes the results obtained just by using spherical correlation, without the last step that utilizes ICP; ρi denotes the final result after all steps of our registration algorithm (a). Angle Θ between known and calculated rotation (b). Distance *d* between known and calculated translation (c).

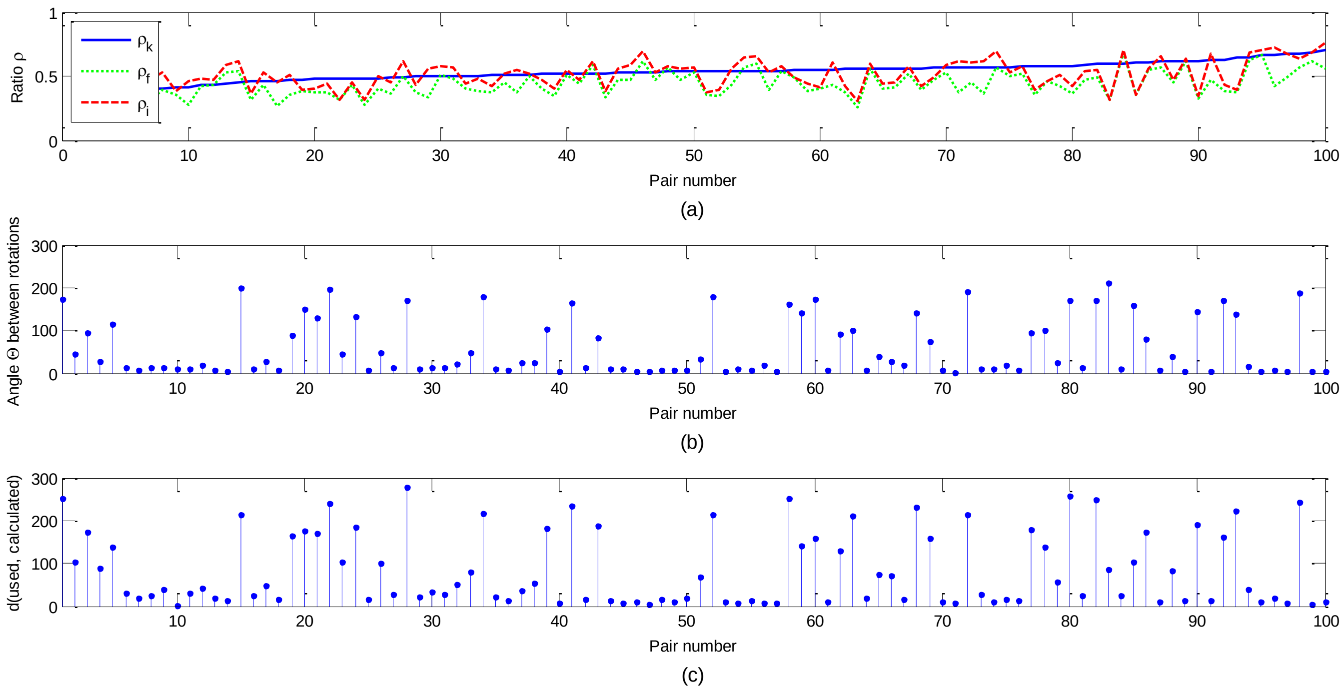

Figure 10: Registration accuracy for 100 volume pairs when all non-rigid changes apply: ρk denotes the results obtained by the same transformation parameters as used in the model creation, ρf denotes the results obtained just by using spherical correlation, without the last step that utilizes ICP; ρi denotes the final result after all steps of our registration algorithm (a). Angle Θ between known and calculated rotation (b). Distance *d* between known and calculated translation (c).